Binding of NO and CO to the d_1 Heme of cd_1 Nitrite Reductase from *Pseudomonas aeruginosa*†

Tapan Kanti Das,‡,§ Emma K. Wilson,‖,⊥ Francesca Cutruzzolà,‖ Maurizio Brunori,‖ and Denis L. Rousseau*,‡

Department of Physiology and Biophysics, Albert Einstein College of Medicine, 1300 Morris Park Avenue, Bronx, New York 10461, and Dipartimento di Scienze Biochimiche, Università di Roma "La Sapienza", P. le A. Moro, 5-00185 Roma, Italy

Received October 4, 2000

ABSTRACT: The cd_1 nitrite reductase, a key enzyme in bacterial denitrification, catalyzes the one-electron reduction of nitrite to nitric oxide. The enzyme contains two redox centers, a *c*-type heme and a unique d_1 heme, which is a dioxoisobacteriochlorin. Nitric oxide, generated by this enzymatic pathway, if not removed from the medium, can bind to the ferrous d_1 cofactor with extremely high affinity and inhibit enzyme activity. In this paper, we report the resonance Raman investigation of the properties of nitric oxide and carbon monoxide binding to the d_1 site of the reduced enzyme. The Fe−ligand (Fe−NO and Fe−CO) stretching vibrational frequencies are unusually high in comparison to those of other ferrous heme complexes. The frequencies of the Fe−NO and N−O stretching modes appear at 585 and 1626 cm^{-1}, respectively, in the NO complex, while the frequencies of the Fe−CO and C−O stretching modes are at 563 and 1972 cm^{-1}, respectively, for the CO complex. Also, the widths (fwhm) of the Fe−CO and C−O stretching modes are smaller than those observed in the corresponding complexes of other heme proteins. The unusual spectroscopic characteristics of the d_1 cofactor are discussed in terms of both its unique electronic properties and the strongly polar distal environment around the iron-bound ligand. It is likely that the influence of a highly ruffled structure of heme d_1 on its electronic properties is the major factor causing anomalous Fe−ligand vibrational frequencies.

In the absence of oxygen, denitrifying bacteria are able to generate energy from phosphorylation processes that involve the reduction of nitrogen oxides. This metabolic pathway, dissimilatory denitrification, involves both membrane-bound and soluble redox proteins (for recent reviews, see refs *1*−*3*). Nitrite reductase (NiR) is a key enzyme in the denitrifying chain where it catalyzes the one-electron reduction of nitrite to form nitric oxide (NO). It has been shown that NiRs fall into two distinct classes depending on the specific redox centers that are present. One class contains copper, and the other contains two heme cofactors (cd_1 NiR) (for reviews, see refs *2*−*4*).

The homodimeric cd_1 NiR (subunit molecular mass of 60 kDa) from the Gram-negative bacterium *Pseudomonas aeruginosa* contains a *c*-type heme, which accepts electrons from external donors such as cytochrome c_{551} (*5*−*7*), and a d_1 heme, which is the site of substrate binding and catalysis (*6*, *8*). To date, the d_1 heme has only been found in cd_1 NiR. This unusual heme is a dioxoisobacteriochlorin with partial saturation in two of its carbonyl-containing pyrrole rings (Figure 1) (*9*). The *c* heme is always low-spin and hexacoordinated with histidine and methionine as its axial ligands (*10*−*12*), whereas the ferric d_1 heme is low-spin and hexacoordinate with a proximal histidine and a distal hydroxide as its axial ligands. However, upon reduction it becomes high-spin and pentacoordinate, allowing facile substrate binding (*10*−*13*). In line with many other heme proteins, a variety of ligands are able to bind to the d_1 heme in both the ferric and ferrous oxidation states. Ligands such as nitric oxide and carbon monoxide bind to the reduced d_1 heme and form stable complexes (*6*, *8*, *14*−*16*).

The catalytic pathway for the conversion of nitrite to NO has not yet been established. It is postulated that following substrate binding, the ferrous d_1 heme donates an electron to nitrite and one oxygen atom is removed by a protonation reaction followed by dehydration (*13*, *17*). This results in the formation of a ferric d_1−NO complex; the dissociation of NO before re-reduction of the d_1 heme (via the *c* heme) is a critical step in catalysis. It has been suggested that the ferric−NO species is an on-pathway intermediate as this derivative is less stable than the ferrous derivative and can release NO more readily; moreover, such a ferric−NO species can be generated in vitro by reacting NO with oxidized cd_1 nitrite reductase (*17*, *18*). Recently, George et al. (*19*) reported the detection of a ferric heme d_1−NO complex by time-resolved infrared spectroscopy in the reaction of the fully reduced enzyme with nitrite. If the

† This work was supported by NIH Grants GM54806 and GM54812 to D.L.R., by CNR of Italy (Target Project on Biotechnology, to F.C.), and by MURST of Italy (P. N. Biologia Strutturale 1999) to M.B. E.K.W. is the recipient of a Human Frontiers Science Program Organization long-term research fellowship.

* To whom correspondence should be addressed. Telephone: (718) 430-4264. Fax: (718) 430-8808. E-mail: rousseau@aecom.yu.edu.

‡ Albert Einstein College of Medicine.

§ Present address: Large Scale Proteomics Corp., 20451 Goldenrod Lane, Germantown, MD 20876.

‖ Università di Roma "La Sapienza".

⊥ Present address: Trends in Biochemical Sciences, Elsevier Science London, 84 Theobald's Rd., London WC1X 8RR, U.K.

10.1021/bi002327i CCC: $20.00
Published on Web 08/14/2001

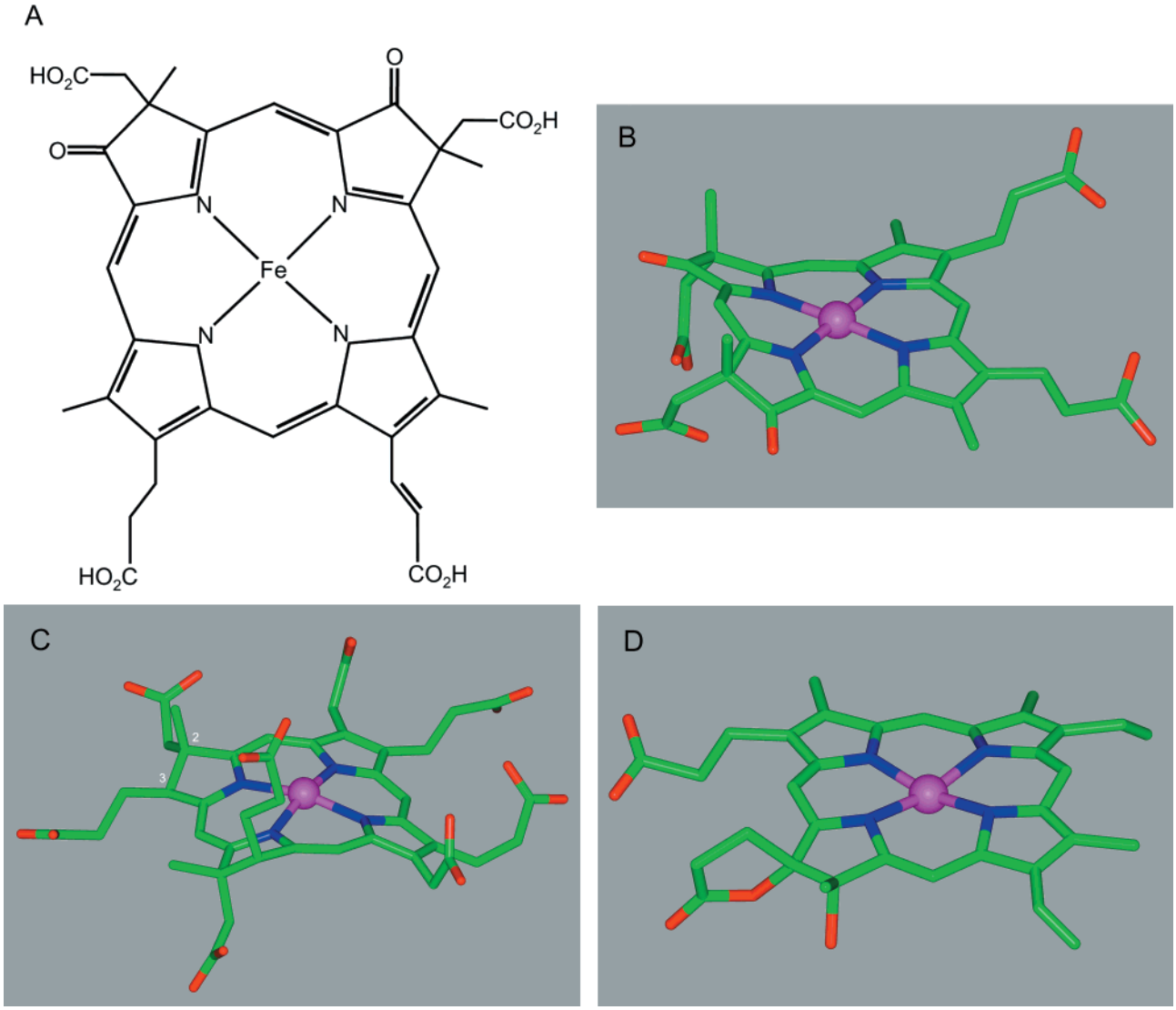

FIGURE 1: (A) Chemical structure of heme d_1. (B) Stereochemical structure of heme d_1 (PDB entry 1nno), showing the severe nonplanarity of the dioxoisobacteriochlorin ring. For comparison, structures of siroheme of sulfite reductase (C) (PDB entry 1aop) and heme *d* of catalase HPII (D) (PDB entry 1gge) are also shown. Heme d_1 and siroheme (both are isobacteriochlorins) are more strongly ruffled than heme *d*. It may be noted that in heme d_1 (B), siroheme (C), and heme *d* (D), the proximal ligands are histidine, cysteine, and tyrosine, respectively (not shown).

ferrous d_1−NO complex is formed, the enzyme becomes locked into a "dead-end" species, due to the very slow dissociation of NO from this adduct (*2*, *6*, *8*). Thus, under certain conditions, nitrite reductase is prone to undergoing severe product inhibition. Although the ferrous−NO species should not be significantly populated in the productive enzymatic cycle, this derivative has been identified in many spectroscopic studies when nitrite is added to nitrite reductase (*6*, *8*, *20*, *21*). The ferrous−NO species has also been observed by stopped-flow kinetic studies, and although this adduct is not catalytically competent, the characterization of its formation is important in establishing the conditions under which the "kinetic trap" is populated (*8*).

The NO and CO adducts of ferrous d_1 bear a strong resemblance to the corresponding derivatives in other heme proteins, such as hemoglobin and myoglobin. As in nitrosylhemoglobin, the d_1−NO species has a $S = {}^1/_2$ ground state and is readily detected by EPR spectroscopy. Resonance Raman spectroscopy has proven to be a very powerful technique for the study of CO and NO derivatives of heme proteins. In particular, the frequencies of the Fe−ligand stretching modes are sensitive to the nature of the heme and the environment in the distal pocket as well as to the nature of the proximal ligand. Furthermore, in the CO complexes, an inverse correlation of the stretching frequencies (thus, the bond orders) between the Fe−CO and C−O stretching modes has been established. Although the ferrous d_1−NO complexes are frequently compared with those of hemoglobin and myoglobin, one has to keep in mind that the d_1 cofactor is a dioxoisobacteriochlorin and therefore is expected to have electronic properties different from those of other hemes. In this study, we have shown that the stretching frequencies of the NO and CO adducts are unique and indeed very different from those of other heme proteins.

EXPERIMENTAL PROCEDURES

Purification of Nitrite Reductase. Nitrite reductase from *P. aeruginosa* was purified according to the method of Parr and co-workers (*22*). The preparation was judged to be pure when the oxidized enzyme had a 411 nm/280 nm absorbance

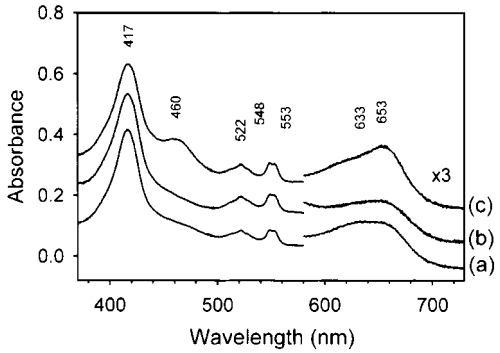

FIGURE 2: Optical spectra of the NO (a) and CO (b) complexes of reduced cd_1 nitrite reductase. The spectrum of the ligand-free reduced enzyme (c) is also shown for comparison. The optical spectra were measured on the same sample that was used for Raman experiments. Reduction was carried out under anaerobic conditions by addition of aliquots of either ascorbate or dithionite in 100 mM sodium phosphate buffer (pH 7.4).

ratio of 1.1. The protein concentration (referenced to the concentration of the active sites) was determined using either an ϵ_{411} of 141 mM^{-1} cm^{-1} or an ϵ_{640} of 20.5 mM^{-1} cm^{-1} for the oxidized protein.

Resonance Raman Spectroscopy. The excitation source for the Raman experiments was the 441.6 nm beam from a CW He−Cd laser (Liconix, Santa Clara, CA). The sample cell (quartz, 2 mm path length, sample volume of ~150 μL) into which a laser beam was focused was spun at 3000−6000 rpm to minimize local heating. The sample cells are custom designed for strict anaerobic measurements and also for recording the optical spectra (UV-2100U spectrophotometer, Shimadzu, Kyoto, Japan) of the same sample for which the Raman spectra are obtained. The Raman scattered light was focused onto the entrance slit (100 μm) of a polychromator (Spex, Metuchen, NJ) and was dispersed by a 1200 grooves/mm grating prior to its detection by a liquid nitrogen-cooled charge-coupled device (CCD) (Princeton Instruments, Trenton, NJ). A Holographic notch filter (Kaiser, Ann Arbor, MI) was used to eliminate Rayleigh scattering. Typically, several 30 s spectra were recorded and averaged. Frequency shifts in the Raman spectra were calibrated using acetone/CCl_4 (for the 100−1000 cm^{-1} region), indene (for the 100−1700 cm^{-1} region), or acetone/potassium ferrocyanide (for the 1700−2400 cm^{-1} region) as a reference. The accuracy of the Raman shifts is approximately ±2 cm^{-1} for absolute shifts and approximately ±0.50 cm^{-1} for relative shifts.

The concentration of the protein samples used for the Raman measurements was ~50 μM in 100 mM phosphate buffer (pH 7.4). Reduction of nitrite reductase was carried out using either buffered ascorbate or dithionite under anaerobic conditions. The nitric oxide derivatives were prepared by injecting either $^{14}N^{16}O$ or $^{15}N^{16}O$ (~99.4% from ICON, Mt. Marion, NY) gas into the solution of reduced nitrite reductase. Similarly, the carbon monoxide complexes were prepared by the addition of either $^{12}C^{16}O$ or $^{13}C^{18}O$ (~99.9% from ICON) gas to the solution of reduced nitrite reductase.

RESULTS

The reduced form of the heme d_1 in nitrite reductase binds diatomic π-acid ligands such as CO and NO and forms very stable complexes (*6*, *8*, *14*−*16*). Figure 2 shows the optical

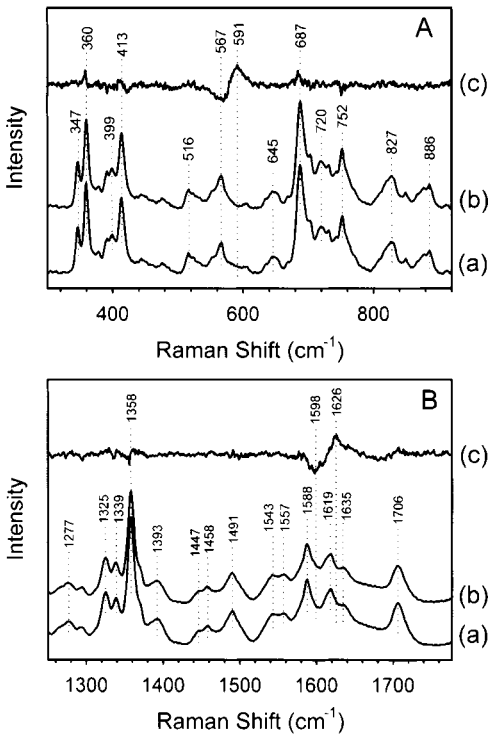

FIGURE 3: Resonance Raman spectra of the NO complex of reduced cd_1. Under the experimental conditions used here [100 mM phosphate (pH 7.4)], NO binds to the d_1 heme only. The spectra shown are for the nitrite reductase adducts of $^{14}N^{16}O$ (a) and $^{15}N^{16}O$ (b) and the difference ($^{14}N^{16}O - {}^{15}N^{16}O$) (c) in the low-frequency region (A) and in the high-frequency region (B).

spectra of the NO and CO complexes in the Soret and visible region in comparison to that of the ligand-free form. The reduced heme *c* in the enzyme has bands at 417 and 522 nm and a doublet at 548/553 nm, which correspond to the transitions in reduced cytochrome *c*. Neither NO nor CO binds to heme *c* under the experimental conditions that were used; however, at pH <6, heme *c* is known to bind NO (*6*). The optical spectrum of the NO-bound d_1 heme consists of a very weak shoulder at ~457 nm, and two broad bands at ~633 and ~653 nm. The CO-bound complex has a very weak shoulder at ~452 nm and a broad band at ~653 nm. The ligand-free reduced form exhibits a relatively more intense Soret band at 460 nm and a visible region band at 654 nm.

The low-frequency region of the resonance Raman spectra of heme proteins is comprised of several in-plane and out-of-plane vibrational modes of the heme, including the ligand vibrational modes. The vibrational modes due to the metal-bound axial ligands are enhanced by electronic coupling of the orbitals of the ligand to the metalloporphyrin electronic orbitals. Assignment of a ligand vibrational mode is extremely useful as it directly identifies a particular ligand and the nature of its interactions with amino acid residues in the heme pocket.

The resonance Raman measurements of cd_1, using a 413.1 nm excitation source, predominantly resulted in the enhancement of the heme *c* vibrational modes. However, when the 441.6 nm excitation source was used, the vibrational modes due to heme d_1 could be observed. Figure 3 shows the spectra of the NO complex of reduced nitrite reductase. To identify the modes involving NO, the $^{14}N^{16}O$ minus $^{15}N^{16}O$ difference spectrum was obtained. Although, the lines could not be

identified in the absolute low-frequency spectra, in the difference spectrum broad features displaying a maximum at ~591 cm^{-1} and a minimum at ~567 cm^{-1} were observed (Figure 3A). A similar isotope frequency shift of ~25 cm^{-1} was observed for the Fe−NO stretching mode (ν_{Fe-NO}) in MbNO by Tomita et al. (*23*). It was noted by them (*23*) and by others (*24*) in the past that for small shifts of broad lines, the peak and the trough in the difference spectra have a larger frequency separation than the authentic separation of the modes in the absolute spectra. It then becomes necessary to either calculate the true frequency shift from the line widths, if available, or carry out simulations. In this case, because the line is so weak and overlapped with porphyrin modes, we are unable to determine precisely the absolute position. For an Fe−NO diatomic model, a 6 cm^{-1} frequency shift is predicted for the $^{14}N^{16}O$ to $^{15}N^{16}O$ comparison for a linear structure, whereas for a highly bent moiety, a 16 cm^{-1} shift is predicted. In MbNO, a large shift was detected (*23*), consistent with a bent structure. We assume that this is also the case here on the basis of the structure (*21*) of nitrite reductase from *P. aeruginosa* (vide infra) and assign the frequency of ν_{Fe-NO} to ~585 cm^{-1} for $^{14}N^{16}O$. Our assignment of this line as ν_{Fe-NO} in nitrite reductase is consistent with that in other heme proteins (*23*, *25*−*28*), although the ν_{Fe-NO} in the present case appears at a higher frequency than that in other heme proteins. We do not detect a line that we can assign as the bending mode. The N−O stretching frequency (ν_{N-O}) was detected at 1626 cm^{-1}, and it shifted to 1598 cm^{-1} upon isotope replacement (Figure 3B). A similar magnitude of the isotope ($^{14}N/^{15}N$) shift was observed for the N−O stretching mode of the ferrous NO complex of myoglobin (*23*). The isotope shift (28 cm^{-1}) in the N−O stretching line at 1626 cm^{-1} is very close to the predicted diatomic (N−O) value of 29 cm^{-1}.

The resonance Raman spectra of the CO complex are shown in Figure 4. The line at 563 cm^{-1} (spectrum a, Figure 4A) with $^{12}C^{16}O$ shifts to 555 cm^{-1} with the $^{13}C^{18}O$ isotope (spectrum b). The 563 cm^{-1} line apparently overlaps with another vibrational mode, probably arising from heme d_1, resulting in residual intensity at this frequency with the isotope. In the difference spectrum, the CO-sensitive lines can be clearly seen by the 563/552 cm^{-1} difference feature. Thus, the Fe−CO stretching frequency is assigned at 563 cm^{-1}. The magnitude of the isotope shift (<11 cm^{-1}) of the 563 cm^{-1} line is consistent with its assignment as a stretching mode, and not a bending mode. Were it a bending mode, the expected isotope shift would be much larger (typically ~20 cm^{-1}). It is to be noted that the Fe−CO stretching mode appears as a very sharp line (fwhm ~ 11.7 cm^{-1}), judged from spectra b and c of Figure 4A, in comparison to that in the CO complex of most other heme proteins (fwhm ~ 20 cm^{-1}). The C−O stretching frequency is identified by the 1972/1881 cm^{-1} feature in the difference spectrum in the 1700−2200 cm^{-1} region as shown in Figure 4B. The line at 1972 cm^{-1} that we assign as the C−O stretching mode is narrower (fwhm ~ 6−7 cm^{-1}) than the C−O stretching frequencies in most hemoglobins and myoglobins (typically, fwhm ~ 10−12 cm^{-1}).

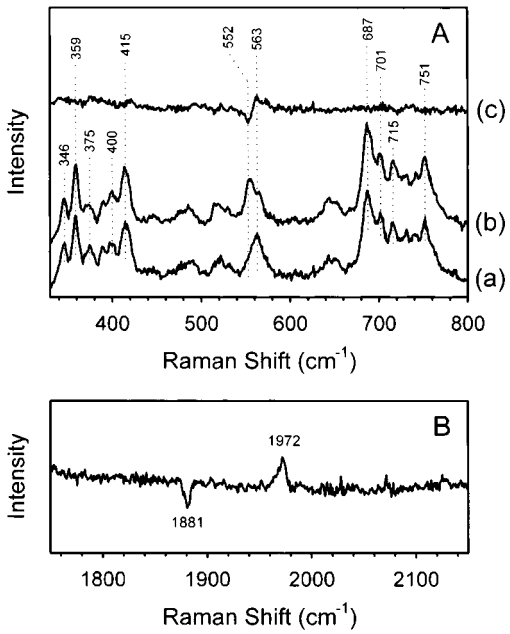

FIGURE 4: Resonance Raman spectra of the CO complex of reduced cd_1. CO is bound to heme d_1 only. (A) The spectra shown in the low-frequency region are for nitrite reductase with $^{12}C^{16}O$ (a) and with $^{13}C^{18}O$ (b) and the difference ($^{12}C^{16}O - {}^{13}C^{18}O$) (c). (B) The difference spectra ($^{12}C^{16}O - {}^{13}C^{18}O$) in the 1700−2200 cm^{-1} region.

DISCUSSION

Nitrite reductase can reduce nitrite to NO in the presence of electron donors, which can be either macromolecules (such as cytochrome c_{551}) or nonphysiological donors, such as ascorbate (*6*, *8*). The electron is first transferred to heme *c* and subsequently to heme d_1 in a slow reaction (*8*, *29*). Finally, nitrite is reduced to NO by the d_1 heme, and the NO is released. However, under certain conditions, the enzyme produces a reduced NO-bound heme d_1 that is a dead-end product (*6*, *8*, *20*, *21*). Thus, it is important to characterize the reduced ligand-bound states. While a large number of CO-bound heme protein complexes have been studied by resonance Raman spectroscopy, the study of NO-bound heme proteins has been limited. In this work, we found that the spectroscopic characteristics of the NO and CO complexes of ferrous cd_1 nitrite reductase are distinct from the analogous complexes of other heme proteins and consistent with the formation of very tightly bound ligands in the ferrous derivatives. The anomalous vibrational properties of the FeXY (XY = CO or NO) group in cd_1 nitrite reductase will be discussed below in relation to the unique electronic nature of heme d_1.

Structure of Heme d_1. The d_1 heme in cd_1 nitrite reductase differs from other iron porphyrins and iron chlorins. Moreover, although the d_1 heme is an isobacteriochlorin, it is different from the isobacteriochlorin of sulfite reductase. In the latter, the macrocycle is a siroheme that has two adjacent partially saturated pyrrole rings (pyrroline) just as in cd_1, but its peripheral groups are very different from those of d_1 heme. Siroheme contains two unsaturated pyrrole rings each with an acetate and propionate at positions 2 and 3, and two partially saturated pyrrole rings each also having an acetate and propionate group and with an additional methyl group at the acetate-carrying carbon (*30*). Heme d_1, on the other hand, contains an oxo group (ketone) at position 3 of each of the two partially saturated pyrrole rings. Additionally, in each of the two unsaturated pyrrole rings, position 2 is occupied by a methyl group, and position 3 contains a

propionate in one and an acrylate in the other. The presence of two partially saturated pyrroles in isobacteriochlorins is likely to account for the origin of the significant distortion of the macrocycle that is evident from the crystal structures of the d_1 heme. See Figure 1 for a comparison between heme d_1, siroheme, and heme *d* from catalase. The macrocycle distortion is most severe in heme d_1. Additional contributions to the distortion may come from perturbations of the π-electron density due to conjugation of the two keto groups and the acrylate moiety.

Chlorins contain only one partially saturated pyrrole ring. For example, the heme *d* in catalase HPII from *Escherichia coli* has a *cis*-hydroxychlorin γ-spirolactone structure (*31*), and it is less ruffled than either siroheme or heme d_1 (Figure 1). In comparison to a planar metalloporphyrin with D_{4h} symmetry, the metallochlorin core has reduced symmetry, C_2. As a result, metallochlorins exhibit additional vibrational modes; however, many of its skeletal modes closely correspond to those of metalloporphyrins (*32*−*34*). Furthermore, the interactions between the iron and the axial ligands have been proposed (*33*) to be similar in iron porphyrins and iron chlorins; thus, the Fe−axial ligand frequencies tend to be in the same frequency range, but they are modulated by the specific properties of the macrocycle.

CO Adducts. CO binds to heme proteins only in their ferrous oxidation state and generally assumes a nearly linear Fe−C−O structure. The general factors that influence the frequencies of the Fe−XY and X−Y stretching modes (XY = CO or NO) are reasonably well understood, but the subtle features remain to be resolved. While the extent to which the steric properties of the Fe−XY moiety can influence the stretching vibrations has not been established, the polarity around the Fe−XY moiety plays a very significant role in determining the Fe−XY and X−Y stretching frequencies. The Fe−CO stretching frequency (ν_{Fe-CO}) in sperm whale myoglobin appears at 509 cm^{-1}; when the distal histidine is replaced with noninteracting groups, the frequency drops to ~495 cm^{-1} (see, for example, refs *35*−*40*). On the other hand, one distal pocket mutant of sperm whale myoglobin, Val68Asn, exhibits a significant increase in the frequency of ν_{Fe-CO}, to 526 cm^{-1} due to an increase in polarity from the asparagine substitution (*39*, *40*). It has been shown that a positively charged or polar environment around CO increases the frequency of ν_{Fe-CO} while a negatively charged or nonpolar environment decreases it (*35*−*43*). Accordingly, a low ν_{Fe-CO} frequency (472 cm^{-1}) in the CO complex of one preparation of guanylate cyclase has been proposed to be due to the presence of a negatively charged group near the CO (*44*). Studies of the CO complexes of several heme proteins have established that there is an inverse correlation between the frequencies of ν_{Fe-CO} and ν_{C-O} (Figure 5). The inverse correlation holds because of the π-acceptor ability of CO, resulting in back-donation of d_π electrons from Fe^{2+} to the empty π^* orbital of CO. Thus, a positive change in the Fe−CO stretching frequency results in a negative change in the frequency of the C−O stretching. The correlation holds for heme proteins containing either histidine or cysteine as proximal ligands with a wide range (472−543 cm^{-1}) of ν_{Fe-CO} values. The difference between the histidine and the cysteine correlation curves is due to greater electron density on the thiolate anion, as compared to histidine, weakening the Fe−C σ bond by competing for the Fe^{2+} dz^2 orbital. The back-bonding phenomenon is not observed when the proximal ligand is either weak or absent; however, the Fe−C σ bond strength is increased in those cases. Additionally, in the case of cytochrome *c* oxidase, the inverse correlation is not observed because of steric interactions with Cu_B, which have been postulated to compress both the Fe−C and C−O bonds, resulting in an increase in ν_{Fe-CO} as well as ν_{C-O} (*45*).

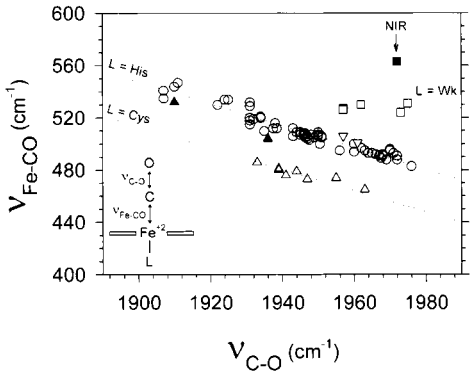

FIGURE 5: Inverse correlation plot of the Fe−CO (ν_{Fe-CO}) and C−O (ν_{C-O}) stretching frequencies. The points denoted with circles are for various hemoglobins, myoglobins, and peroxidases that contain histidine as their proximal ligand (L). It also includes a few points that represent model heme *d* (chlorin) complexes (▽). The black square denotes cd_1 nitrite reductase. The upward triangles (△) are for different cytochrome P450s that have cysteine as a proximal ligand. The black upward triangles (▲) are for siroheme of sulfite reductase that also has a cysteine as a proximal ligand. In the case of a weak proximal ligand or the absence of a proximal ligand (□), no correlation is observed. The dotted lines represent a linear regression analysis through each set of points.

The Fe−CO stretching mode of nitrite reductase appears at a frequency (563 cm^{-1}) higher than that of any known Fe^{2+}−CO heme complex. It is well established that a strong polar environment around the CO increases the frequency of the Fe−CO stretching mode. The distal pocket of the d_1 heme in fact contains three polar residues, His369, His327, and Tyr10 (*13*, *21*). Hydrogen bonding between the heme d_1-bound ligands and the two histidines and the tyrosine has been proposed to be critical in various steps of the catalytic cycle of nitrite reductase (*17*). It should also be noted that the widths (fwhm) of the Fe−CO and C−O bands are smaller than those of the corresponding bands in CO complexes of many heme proteins. One possible reason is that the CO is held in a very structured distal pocket due to interactions with the distal pocket residues that are organized by an extensive H-bonding network (*13*, *46*). This is consistent with the observation of a slow rate of CO dissociation (0.03−0.041 s^{-1}) from the CO complex of this enzyme (*14*, *15*).[1] The strong positive polarity in the distal pocket (Figure 6) is expected to enhance the back-bonding, resulting in an increased frequency of the Fe−CO bond and a concomitant decrease in the C−O stretching mode. However, the C−O stretching mode is located at 1972 cm^{-1}, a very high frequency. Consequently, the CO adduct of nitrite reductase does not lie on the inverse correlation curve relating the Fe−

[1] Parr and co-workers measured the dissociation rate constant for CO by using NO and O_2 to displace CO from the ascorbate-reduced CO complex, and observed biphasic kinetics with rate constants of 0.03 and 0.15 s^{-1} (*14*). However, Wharton and Gibson (*15*) estimated a dissociation rate of 0.041 s^{-1} with the dithionite-reduced enzyme, whereas the model used by Wilson et al. (*16*) yielded a rate of 0.12 s^{-1}.

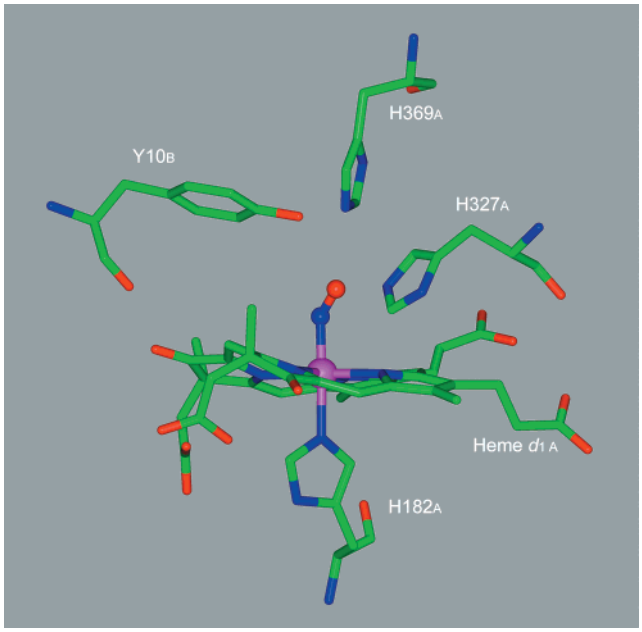

FIGURE 6: Structure of the NO-bound d_1 heme of cd_1 nitrite reductase from *P. aeruginosa* (PDB entry 1nno). Only selective residues around the d_1 heme of one monomer (designated as A) are shown. His182 is the proximal histidine. The distal pocket contains two histidine residues (His369 and His327 which are 2.6 and 3.4 Å, respectively, from the oxygen of NO) of the same monomer and one tyrosine residue (4.2 Å from the oxygen of NO) of the second monomer (B).

CO and C−O stretching frequencies (Figure 5). Instead, it falls at a much higher position in the diagram, far from the correlation line for proximal histidine-containing heme proteins, although the proximal ligand of heme d_1 is a histidine (His182). Steric factors, distorting the CO, do not appear to play a role in significantly affecting the frequency since in the closely related nitrite reductase from *Paracoccus denitrificans*, the Fe−C−O moiety was only slightly bent away from normal to the heme (*46*).

We propose that the displacement of the CO adduct from the Fe−CO versus C−O correlation curve is due to the difference in the electronic properties of heme d_1 compared to other hemes. The ruffled structure of *isobacteriochlorins* affects the overlap between the orbitals of the metal and the macrocycle. Thus, the balance between equatorial and axial π back-bonding in the CO complex is very different from that in iron porphyrins. As a result, the Fe−C−O frequencies of cd_1 do not fall on the ν_{Fe-CO} versus ν_{C-O} correlation line. On the other hand, the balance between equatorial and axial π back-bonding in iron *chlorins* appears to be similar to that in iron porphyrins; thus, most chlorins lie on the inverse correlation curve (Figure 5) relating the Fe−CO and C−O stretching frequencies (*32*), consistent with the suggestions of Kitagawa and Ozaki (*33*). It may be noted that the Fe−CO and C−O frequencies (*47*) of the CO complex of the siroheme (also an isobacteriochlorin with a strongly ruffled structure as shown in Figure 1, but in which the proximal ligand is cysteine) in sulfite reductase also do not fall on the correlation line of cysteine-containing heme proteins (Figure 5), although CO binds in a nearly linear fashion (*30*).

NO Adducts. In contrast to the well-established back-bonding correlation in CO derivatives of heme proteins, it has not been established yet if a back-bonding correlation

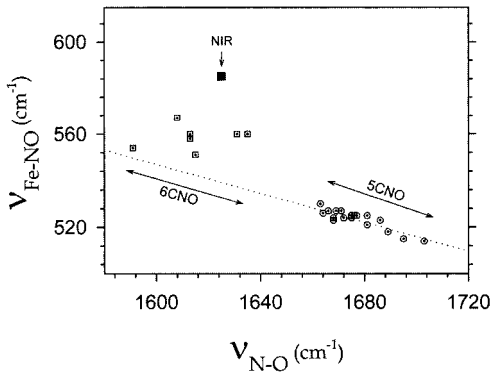

FIGURE 7: Plot relating the Fe−NO (ν_{Fe-NO}) and N−O (ν_{N-O}) stretching frequencies. The circles are for five-coordinate heme−NO complexes, and the squares are for six-coordinate NO complexes of heme proteins. The black square denotes the ferrous NO complex of cd_1 nitrite reductase.

between Fe−NO and N−O stretching frequencies exists in *hexacoordinated* NO complexes of heme proteins. An inverse relationship between the Fe−NO and N−O frequencies was reported recently (*48*) in *pentacoordinate* NO ferrous complexes of model hemes (*48*−*50*) containing different peripheral substituents (see Figure 7). Although neither the effect of the distal residues nor the proximal factor on Fe−NO or N−O frequencies was determined in that study (*48*), it is clear that a change in the electron density in the porphyrin ring that affects the bond order of the Fe−NO species concomitantly alters the N−O bond order in the pentacoordinate NO complexes and yields a reasonable inverse correlation. The scattered nature of the limited number of data points that are available for the hexacoordinate NO ferrous complexes (Figure 7) makes the back-bonding correlation between Fe−NO and N−O bond orders in hexacoordinate complexes uncertain.

The NO complex of reduced nitrite reductase shows unusual vibrational frequencies just as the CO derivative displayed unusual frequencies. The ν_{Fe-NO} mode appears at a higher frequency (585 cm^{-1}) than those in the ferrous NO complexes of other heme proteins (*23*, *25*−*28*, *44*, *51*−*56*). Although the frequency of ν_{Fe-NO} for the His-Fe−NO structure is known only for a limited number of heme proteins (*23*, *25*−*28*, *51*−*54*), they are all clustered at ∼560 cm^{-1} (Figure 7). The ν_{N-O} values in these complexes (∼1590−1640 cm^{-1}) (*23*, *25*−*28*, *51*−*54*, *57*), however, are spread out, and that of nitrite reductase (1626 cm^{-1}) falls in the middle of the distribution. The pentacoordinate ferrous heme−NO complexes show distinct frequencies from the hexacoordinate complexes as shown in Figure 7. Surprisingly, the frequency of ν_{Fe-NO} in *ferrous* nitrite reductase is very similar to that in the *ferric* heme−NO moieties of myoglobin (595 cm^{-1}) and other heme proteins (*26*) and model heme complexes (∼600 cm^{-1}) (*49*), although the frequency of ν_{N-O} in globins and other heme proteins is observed at a much higher frequency (∼1927 cm^{-1}) (*58*, *59*). The crystal structure of the NO complex of reduced nitrite reductase shows that NO is surrounded by three polar residues (His369, His327, and Tyr10) and is strongly hydrogen bonded to His369 at a distance of 2.6 Å (*21*). Such an arrangement in the distal pocket would be expected to exert a strong polar effect on the Fe-bound NO, and could increase the Fe−NO bond order just as in Fe−CO com-

plexes. A possible steric effect must also be considered. However, the crystal structure of the ferrous NO form of nitrite reductase from *P. aeruginosa* shows that the Fe−N−O angle is 135° (*21*). This is similar to that observed in NO derivatives in heme proteins (*60*, *61*) and model complexes (*62*), and consequently, no large change in the geometry expected from electronic structure considerations occurs in the complex. Thus, the observation that the nitrite reductase NO complex is positioned at a much higher value in the ν_{Fe-NO} versus ν_{N-O} plot (Figure 7) suggests that the distinct structure of heme d_1 causes unusual frequencies of Fe−NO stretching just as in the case of Fe−CO stretching discussed in the preceding section. A strong Fe−NO bond identified in this study is highly consistent with the formation of a dead-end NO complex of the enzyme observed in several studies.

CONCLUSIONS

The anomalously high frequencies of Fe−CO and Fe−NO stretching in the cd_1 nitrite reductase of *P. aeruginosa* suggest that the unique electronic nature of heme d_1 in comparison to other hemes plays a significant role in determining the vibrational properties. The unique electronic nature of heme d_1 is reflected in its strongly ruffled structure. The high frequencies for the Fe−CO and Fe−NO stretching modes indicating strong bonding of the exogenous ligands to the heme d_1 provide a clue as to why the ferrous−NO complex is formed under a variety of in vitro experimental conditions and the enzyme is strongly inhibited. Thus, a delicate balance between electron transfer and ligand channeling is extremely important in cd_1 in maintaining continued enzymatic function. It is also possible that formation of the NO-inhibited complex could serve as an effective autoinhibitory control on the enzymatic activity just as that proposed for nitric oxide synthase (*63*).

REFERENCES

1. Zumft, W. G. (1997) Cell biology and molecular basis of denitrification, *Microbiol. Mol. Biol. Rev. 61*, 533−616.
2. Averill, B. A. (1996) Dissimilatory nitrite and nitric oxide reductases, *Chem. Rev. 96*, 2951−2964.
3. Cutruzzolà, F. (1999) Bacterial nitric oxide synthesis, *Biochim. Biophys. Acta 1411*, 231−249.
4. Silvestrini, M. C., Falcinelli, S., Ciabatti, I., Cutruzzolà, F., and Brunori, M. (1994) *Pseudomonas aeruginosa* nitrite reductase (or cytochrome oxidase): an overview, *Biochimie 76*, 641−654.
5. Kuronen, T., and Ellfolk, N. (1972) A new purification procedure and molecular properties of *Pseudomonas* cytochrome oxidase, *Biochim. Biophys. Acta 275*, 308−318.
6. Silvestrini, M. C., Colosimo, A., Brunori, M., Walsh, T. A., Barber, D., and Greenwood, C. (1979) A re-evaluation of some basic structural and functional properties of *Pseudomonas* cytochrome oxidase, *Biochem. J. 183*, 701−709.
7. Silvestrini, M. C., Tordi, M. G., Colosimo, A., Antonini, E., and Brunori, M. (1982) The kinetics of electron transfer between *Pseudomonas aeruginosa* cytochrome *c*-551 and its oxidase, *Biochem. J. 203*, 445−451.
8. Silvestrini, M. C., Tordi, M. G., Musci, G., and Brunori, M. (1990) The reaction of *Pseudomonas* nitrite reductase and nitrite. A stopped-flow and EPR study, *J. Biol. Chem. 265*, 11783−11787.
9. Chang, C. K., Timkovick, R., and Wu, W. (1986) Evidence that heme d_1 is a 1,3-porphyrindione, *Biochemistry 25*, 8447−8453.
10. Muhoberac, B. B., and Wharton, D. C. (1983) Electron paramagnetic resonance study of the interaction of some anionic ligands with oxidized *Pseudomonas* cytochrome oxidase, *J. Biol. Chem. 258*, 3019−3027.
11. Timkovich, R., and Cork, M. S. (1983) Magnetic susceptibility measurements on *Pseudomonas* cytochrome cd_1, *Biochim. Biophys. Acta 742*, 162−168.
12. Walsh, T. A., Johnson, M. K., Greenwood, C., Barber, D., Springall, J. P., and Thomson, A. J. (1979) Some magnetic properties of *Pseudomonas* cytochrome oxidase, *Biochem. J. 177*, 29−39.
13. Nurizzo, D., Silvestrini, M. C., Mathieu, M., Cutruzzolà, F., Bourgeois, D., Fülöp, V., Hajdu, J., Brunori, M., Tegoni, M., and Cambillau, C. (1997) N-Terminal arm exchange is observed in the 2.15 Å crystal structure of oxidized nitrite reductase from *Pseudomonas aeruginosa*, *Structure 5*, 1157−1171.
14. Parr, S. R., Wilson, M. T., and Greenwood, C. (1995) The reaction of *Pseudomonas aeruginosa* cytochrome *c* oxidase with carbon monoxide, *Biochem. J. 151*, 51−59.
15. Wharton, D. C., and Gibson, Q. H. (1976) Cytochrome oxidase from *Pseudomonas aeruginosa*. IV. Reaction with oxygen and carbon monoxide, *Biochim. Biophys. Acta 430*, 445−453.
16. Wilson, E. K., Bellelli, A., Liberti, S., Arese, M., Grasso, S., Cutruzzolà, F., Brunori, M., and Brzezinski, P. (1999) Internal electron transfer and structural dynamics of cd_1 nitrite reductase revealed by laser CO photodissociation, *Biochemistry 38*, 7556−7564.
17. Fülöp, V., Moir, J. W. B., Ferguson, S. J., and Hajdu, J. (1995) The anatomy of a bifunctional enzyme: structural basis for reduction of oxygen to water and synthesis of nitric oxide by cytochrome cd_1, *Cell 81*, 369−377.
18. Wang, Y., and Averill, B. A. (1996) Direct observation by FTIR spectroscopy of the ferrous heme-NO^+ intermediate in reduction of nitrite by a dissimilatory heme cd_1 nitrite reductase, *J. Am. Chem. Soc. 118*, 3972−3973.
19. George, S. J., Allen, J. W. A., Ferguson, S. J., and Thorneley, R. N. F. (2000) Time-resolved infrared spectroscopy reveals a stable ferric heme-NO intermediate in the reaction of *Paracoccus pantotrophus* cytochrome cd_1 nitrite reductase with nitrite, *J. Biol. Chem. 275*, 33231−33237.
20. Johnson, M. K., Thomson, A. J., Walsh, T. A., Barber, D., and Greenwood, C. (1980) Electron paramagnetic resonance studies on *Pseudomonas* nitrosyl nitrite reductase. Evidence for multiple species in the electron paramagnetic resonance spectra of nitrosyl haemoproteins, *Biochem. J. 189*, 285−294.
21. Nurizzo, D., Cutruzzolà, F., Arese, M., Bourgeois, D., Brunori, M., Cambillau, C., and Tegoni, M. (1998) Conformational changes occurring upon reduction and NO binding in nitrite reductase from *Pseudomonas aeruginosa*, *Biochemistry 37*, 13987−13996.
22. Parr, S. R., Barber, D., Greenwood, C., Phillips, B. W., and Melling, J. (1976) A purification procedure for the soluble cytochrome oxidase and some other respiratory proteins from *Pseudomonas aeruginosa*, *Biochem. J. 157*, 423−430.
23. Tomita, T., Hirota, S., Ogura, T., Olson, J. S., and Kitagawa, T. (1999) Resonance Raman investigation of Fe−N−O structure of nitrosylheme in myoglobin and its mutants, *J. Phys. Chem. B 103*, 7044−7054.
24. Rousseau, D. L. (1981) Raman Difference Spectroscopy as a Probe of Biological Molecules, *J. Raman Spectrosc. 10*, 94−99.
25. Tsubaki, M., and Yu, N.-T. (1982) Resonance Raman investigation of nitric oxide bonding in nitrosylhemoglobin A and -myoglobin: detection of bound N−O stretching and Fe−NO stretching vibrations from the hexacoordinated NO-heme complex, *Biochemistry 21*, 1140−1144.
26. Benko, B., and Yu, N.-T. (1983) Resonance Raman studies of nitric oxide binding to ferric and ferrous hemoproteins: detection of Fe(III)−NO stretching, Fe(III)−N−O bending, and Fe(II)−N−O bending vibrations, *Proc. Natl. Acad. Sci. U.S.A. 80*, 7042−7046.
27. Hu, S., and Kincaid, J. R. (1991) Resonance Raman characterization of nitric oxide adducts of cytochrome P450cam: The effect of substrate structure on the iron-ligand vibrations, *J. Am. Chem. Soc. 113*, 2843−2850.

28. Hu, S., and Kincaid, J. R. (1991) Resonance Raman spectra of the nitric oxide adducts of ferrous cytochrome P450cam in the presence of various substrates, *J. Am. Chem. Soc. 113*, 9760−9766.
29. Parr, S. R., Barber, D., Greenwood, C., and Brunori, M. (1977) The electron-transfer reaction between azurin and the cytochrome *c* oxidase from *Pseudomonas aeruginosa*, *Biochem. J. 167*, 447−455.
30. Crane, B. R., Siegel, L. M., and Getzoff, E. D. (1997) Probing the catalytic mechanism of sulfite reductase by X-ray crystallography: structures of the *Escherichia coli* hemoprotein in complex with substrates, inhibitors, intermediates, and products, *Biochemistry 36*, 12120−12137.
31. Bravo, J., Mate, M. J., Schneider, T., Switala, J., Wilson, K., Loewen, P. C., and Fita, I. (1999) Structure of catalase HPII from *Escherichia coli* at 1.9 Å resolution, *Proteins 34*, 155−166.
32. Sun, J., Chang, C. K., and Loehr, T. M. (1997) Q-Band resonance Raman enhancement of Fe−CO vibrations in ferrous chlorin complexes: possible monitor of axial ligands in *d* cytochromes, *J. Phys. Chem. B 101*, 1476−1483.
33. Kitagawa, T., and Ozaki, Y. (1987) Infrared and Raman spectra of metalloporphyrins, *Struct. Bonding 64*, 73−94.
34. Schick, G. A., and Bocian, D. F. (1987) Resonance Raman studies of hydroporphyrins and chlorophylls, *Biochim. Biophys. Acta 895*, 127−154.
35. Yu, N.-T., and Kerr, E. A. (1988) Vibrational modes of coordinated CO, CN^-, O_2 and NO, in *Biological Application of Raman Spectroscopy* (Spiro, T. G., Ed.) Vol. 3, pp 39−95, John Wiley & Sons, New York.
36. Ray, G. B., Li, X.-Y., Ibers, J. A., Sessler, J. L., and Spiro, T. G. (1994) How far can proteins bend the FeCO unit? Distal polar and steric effects in heme proteins and models, *J. Am. Chem. Soc. 116*, 162−176.
37. Morikis, D., Champion, P. M., Springer, B. A., and Sligar, S. G. (1989) Resonance Raman investigations of site-directed mutants of myoglobin: effects of distal histidine replacement, *Biochemistry 28*, 4791−4800.
38. Ling, J., Li, T., Olson, J. S., and Bocian, D. F. (1994) Identification of the iron−carbonyl stretch in distal histidine mutants of carbonmonoxymyoglobin, *Biochim. Biophys. Acta 1188*, 417−421.
39. Phillips, G. N., Jr., Teodoro, M. L., Li, T., Smith, B., and Olson, J. S. (1999) Bound CO as a molecular probe of electrostatic potential in the distal pocket of myoglobin, *J. Phys. Chem. B 103*, 8817−8829.
40. Anderton, C. L., Hester, R. E., and Moore, J. N. (1997) A chemometric analysis of the resonance Raman spectra of mutant carbonmonoxy-myoglobins reveals the effects of polarity, *Biochim. Biophys. Acta 1338*, 107−120.
41. Das, T. K., Lee, H. C., Duff, S. M., Hill, R. D., Peisach, J., Rousseau, D. L., Wittenberg, B. A., and Wittenberg, J. B. (1999) The heme environment in barley hemoglobin, *J. Biol. Chem. 274*, 4207−4212.
42. Das, T. K., Friedman, J. M., Kloek, A. P., Goldberg, D. E., and Rousseau, D. L. (2000) Origin of the anomalous Fe−CO stretching mode in the CO complex of *Ascaris* hemoglobin, *Biochemistry 39*, 837−842.
43. Kushkuley, B., and Stavrov, S. S. (1996) Theoretical study of the distal-side steric and electrostatic effects on the vibrational characteristics of the FeCO unit of the carbonylheme proteins and their models, *Biophys. J. 70*, 1214−1229.
44. Deinum, G., Stone, J. R., Babcock, G. T., and Marletta, M. A. (1996) Binding of nitric oxide and carbon monoxide to soluble guanylate cyclase as observed with resonance Raman spectroscopy, *Biochemistry 35*, 1540−1547.
45. Das, T. K., Tomson, F. L., Gennis, R. B., Gordon, M., and Rousseau, D. L. (2001) pH-dependent structural changes at the heme-copper binuclear center of cytochrome *c* oxidase, *Biophys. J.* (in press).
46. Sjögren, T., Svensson-Ek, M., Hajdu, J., and Brzezinski, P. (2000) Proton-coupled structural changes upon binding of carbon monoxide to cytochrome cd_1: A combined flash photolysis and X-ray crystallography study, *Biochemistry 39*, 10967−10974.
47. Han, S. H., Madden, J. F., Siegel, L. M., and Spiro, T. G. (1989) Resonance Raman studies of *Escherichia coli* sulfite reductase hemoprotein. 3. Bound ligand vibrational modes, *Biochemistry 28*, 5477−5485.
48. Vogel, K. M., Kozlowski, P. M., Zgierski, M. Z., and Spiro, T. G. (1999) Determinants of the FeXO (X = C, N, O) Vibrational Frequencies in Heme Adducts from Experiment and Density Functional Theory, *J. Am. Chem. Soc. 121*, 9915−9921.
49. Lipscomb, L. A., Lee, B.-S., and Yu, N.-T. (1993) Resonance Raman investigation of nitric oxide bonding in iron porphyrins: Detection of the Fe−NO stretching vibration, *Inorg. Chem. 32*, 281−286.
50. Choi, I.-K., Liu, Y., Feng, D. W., Paeng, K.-J., and Ryan, M. D. (1991) *Inorg. Chem. 30*, 1832−1839.
51. Deng, T. J., Proniewicz, L. M., Kincaid, J. R., Yeom, H., Macdonald, I. D., and Sligar, S. G. (1999) Resonance Raman studies of cytochrome P450BM3 and its complexes with exogenous ligands, *Biochemistry 38*, 13699−13706.
52. Obayashi, E., Takahashi, S., and Shiro, Y. (1998) Electronic structure of reaction intermediate of cytochrome P450nor in its nitric oxide reduction, *J. Am. Chem. Soc. 120*, 12964−12965.
53. Rousseau, D. L., Singh, S., Ching, Y. C., and Sassaroli, M. (1988) Nitrosyl cytochrome *c* oxidase. Formation and properties of mixed valence enzyme, *J. Biol. Chem. 263*, 5681−5685.
54. Lukat-Rodgers, G. S., and Rodgers, K. R. (1997) Characterization of ferrous FixL-nitric oxide adducts by resonance Raman spectroscopy, *Biochemistry 36*, 4178−4187.
55. Tomita, T., Ogura, T., Tsuyama, S., Imai, Y., and Kitagawa, T. (1997) Effects of GTP on bound nitric oxide of soluble guanylate cyclase probed by resonance Raman spectroscopy, *Biochemistry 36*, 10155−10160.
56. Fan, B., Gupta, G., Danziger, R. S., Friedman, J. M., and Rousseau, D. L. (1998) Resonance Raman characterization of soluble guanylate cyclase expressed from baculovirus, *Biochemistry 37*, 1178−1184.
57. Zhao, X. J., Sampath, V., and Caughey, W. S. (1994) Infrared characterization of nitric oxide bonding to bovine heart cytochrome *c* oxidase and myoglobin, *Biochem. Biophys. Res. Commun. 204*, 537−543.
58. Miller, L. M., Pedraza, A. J., and Chance, M. R. (1997) Identification of conformational substates involved in nitric oxide binding to ferric and ferrous myoglobin through difference Fourier transform infrared spectroscopy (FTIR), *Biochemistry 36*, 12199−12207.
59. Sampath, V., Zhao, X. J., and Caughey, W. S. (1994) Characterization of interactions of nitric oxide with human hemoglobin A by infrared spectroscopy, *Biochem. Biophys. Res. Commun. 198*, 281−287.
60. Rich, A. M., Armstrong, R. S., Ellis, P. J., and Lay, P. A. (1998) Determination of the Fe-ligand bond lengths and Fe−N−O bond angles in horse heart ferric and ferrous nitrosylmyoglobin using multiple-scattering XAFS analyses, *J. Am. Chem. Soc. 120*, 10827−10836.
61. Brucker, E. A., Olson, J. S., Ikeda-Saito, M., and Phillips, G. N., Jr. (1998) Nitric oxide myoglobin: crystal structure and analysis of ligand geometry, *Proteins 30*, 352−356.
62. Piciulo, P. L., Rupprecht, G., and Scheidt, W. R. (1974) Stereochemistry of nitrosylmetalloporphyrins. Nitorsyl-α,β,γ,δ-tetraphenylporphinato(1-methylimidazole)iron and nitrosyl-α,β,γ,δ-tetraphenylporphinato(4-methylpiperidine)manganese, *J. Am. Chem. Soc. 96*, 5293−5295.
63. Abu-Soud, H. M., Wang, J., Rousseau, D. L., Fukuto, J. M., Ignarro, L. J., and Stuehr, D. J. (1995) Neuronal nitric oxide synthase self-inactivates by forming a ferrous-nitrosyl complex during aerobic catalysis, *J. Biol. Chem. 270*, 22997−23006.

BI002327I